

AN ABSTRACT OF THE THESIS OF

Nam Hwang for the degree of Master of Science in Electrical and Computer Engineering presented on June 22, 1990. Title: A Dual-Frequency Diode Laser Displacement Sensor

Redacted for Privacy

Abstract approved: _____

Thomas K. Plant

The purpose of this work is to develop an accurate non-contacting displacement sensor for use in industrial environments. The accurate measurement of small displacements is important for many industrial process applications such as lumber sawing, paper production and robot position sensing.

A simple technique for the measurement of small displacements has been developed using semiconductor diode lasers in a heterodyne laser ranging system. Two collimated diode lasers are directly amplitude modulated at f_m and $f_m + f_b$ where f_m is 10 - 300 MHz and f_b is 10 - 50 KHz. One laser beam is reflected off the target and focused onto a detector along with the other (local oscillator) laser beam. A heterodyne signal at the beat frequency (f_b) is produced. Small displacements cause a phase shift between the local oscillator signal and the collected signal from the target. Displacement sensing accuracies of 1.4 μm and 50 nm have been calculated and measured over dynamic ranges of 3.5 m and 1 cm for $f_m = 10$ MHz and 300 MHz, respectively.

It has been shown that using heterodyne laser ranging with diode lasers is an accurate displacement measurement technique for industrial applications.

A Dual-Frequency Diode Laser Displacement Sensor

by

Nam Hwang

A THESIS

submitted to

Oregon State University

in partial fulfillment of
the requirements for the
degree of

Master of Science

Completed June 22, 1990

Commencement June 1991

APPROVED:

Redacted for Privacy

Professor of Electrical and Computer Engineering
in charge of major

Redacted for Privacy

Head of Department of Electrical and Computer Engineering

Redacted for Privacy

Dean of Graduate School

Date thesis is presented June 22, 1990

Written and typed by Nam Hwang

To:

My family

ACKNOWLEDGEMENTS

First of all, I would like to express my sincere thanks to Dr. Thomas K. Plant, my major professor and thesis advisor, for his support, advice, suggestions, and comments through all stages of my research and thesis. The technical and partial financial support on this thesis work from Lucidyne Technologies, Inc. (Mr. Joseph G. LaChapelle) of Corvallis, Oregon is gratefully acknowledged.

Special thanks are due to Mr. Seung-Bae Kim, Dr. Hyung-Mo Yoo, and Mr. Ravindranath. T. Kollipara for their kind assistance through this research work.

TABLE OF CONTENTS

1. INTRODUCTION	1
2. DESIGN PRINCIPLES OF THE SENSOR	4
2.1 Direct Amplitude Modulation	4
2.2 Heterodyne Detection and Beat Frequency	6
2.3 Laser Ranging	13
3. EXPERIMENTS AND RESULTS	17
3.1 Direct Amplitude Modulation of Diode lasers	17
3.1.1. Experiment	17
3.1.2. Results	19
3.2 System Alignment	25
3.3 Optical Heterodyne Detection	25
3.3.1. Experiment	25
3.3.2. Results	27
3.4 Performance Analysis	28
3.4.1. Experiment	28
3.4.2. Results	32
4. DISCUSSION	37
5. CONCLUSIONS	40
BIBLIOGRAPHY	42

LIST OF FIGURES

Fig. 2-1	Block diagram of the design process.	5
Fig. 2-2	Principle of direct amplitude modulation.	7
Fig. 2-3	Schematic diagram of a heterodyne detection system.	8
Fig. 2-4	Plot of maximum unambiguous range versus modulation frequency.	12
Fig. 2-5	Plot of displacement accuracy as a function of heterodyne signal power level.	16
Fig. 3-1	Schematic diagram of experimental setup of a dual-frequency diode laser displacement sensor.	18
Fig. 3-2	Drive circuit for direct amplitude modulation of CD laser diode.	20
Fig. 3-3 (a)	Plot of optical power output versus forward current.	22
Fig. 3-3 (b)	Plot of optical power output versus monitor current.	23
Fig. 3-4	Typical waveforms of direct amplitude modulation.	24
Fig. 3-5	Optical heterodyne detection circuit.	26
Fig. 3-6 (a)	Optical heterodyne detection of the signal and local oscillator light sources by a spectrum analyzer.	29
Fig. 3-6 (b)	Optical heterodyne detection of a beat signal.	30
Fig. 3-7	Optical heterodyne detection output waveforms on an oscilloscope.	31
Fig. 3-8 (a)	Monitored oscilloscope traces ($f_S = 100.00$ MHz, $f_{LO} = 100.01$ MHz, and $dz = 37.5$ cm).	33
Fig. 3-8 (b)	Monitored oscilloscope traces ($f_S = 10.00$ MHz, $f_{LO} = 10.01$ MHz, and $dz = 180$ cm).	34

Fig. 3-9 Plot of displacement versus phase shift
as a function of modulation frequency.

A DUAL-FREQUENCY DIODE LASER DISPLACEMENT SENSOR

1. INTRODUCTION

There has been extensive research in the area of displacement measurement [1]-[17]. The measurement of small displacement is not only important for laser mode control and precision optics such as mirror and lens positioning, but it has also become a very important quality control (QC) technique for many industrial areas [1]-[3]. For example, it is used to increase the quality and quantity of products such as paper, film, sheet metal, and semiconductor wafers. In the case of large space structures such as space stations and space antennas which are flexible and may have active control mechanisms for damping oscillations, returning to normal shape, and reducing stress; one method for monitoring the relative movement of structural elements is a laser displacement measurement system [4].

Optical interferometric methods are well suited to measuring small displacements [2]-[3], [5]-[16]. For example, displacements of a few micrometer can be measured using a Mach-Zehnder interferometer, a stable HeNe laser, and a frequency counter [5]. Because the Mach-Zehnder interferometer is very sensitive to mechanical vibration and misalignment [6], this technique is rather difficult to use. In addition, expensive

equipment such as stable lasers and fast counters are needed. Other techniques for such measurements are basically classified into two categories [11]-[12] : optical homodyne and heterodyne detection processes. The optical homodyne detection process generally uses a Michelson interferometer with one laser split into a reference and a signal beam. The optical heterodyne detection process uses a similar kind of interferometer, but it needs two laser beams of different frequencies (f_m , $f_m + f_b$) to generate a signal photocurrent at the beat frequency (f_b) [13]-[16]. Most laser displacement measurement systems use a pulsed signal and determine distance by the travel time of the laser pulse. For applications at large distances and low resolution (a few meters), pulsed systems are adequate; however, for small displacements at relatively short distances, a continuous wave (CW) modulated signal provides improved resolution [17].

The main advantage of using a heterodyne laser ranging system is that it is non-contacting so that no alteration of the actual surface occurs. It can be used in harsh environments such as for high-temperature processes. Also, it is so sensitive that it has been calculated and tested to have a displacement accuracy of 0.2 μm at $f_m = 300 \text{ MHz}$. Because of the ability to focus the laser beam to a small spot, point-by-point measurements of the surface and complete characterization

of the displacement field are easily accomplished [10], [15].

The goals of this thesis work were

- (1) to review design considerations for establishing a laser ranging sensor, with particular emphasis on direct amplitude modulation and heterodyne detection techniques;
- (2) to present experimental results that support the viability of the dual-frequency diode laser displacement sensor by evaluating its dynamic (unambiguous) range and its displacement measurement accuracy;
- (3) to discuss those emerging concepts that bear on the dual-frequency diode laser displacement sensor.

2. DESIGN CONSIDERATIONS

In this chapter, concepts and theories used in the thesis are briefly reviewed. The general process is illustrated schematically in Fig. 2-1.

2.1 Direct Amplitude Modulation [18]-[22]

An important feature of semiconductor diode lasers is their ability to respond to direct, high speed modulation. The principal attraction of the direct modulation technique is its simplicity. With the laser biased above threshold and a modulation signal superimposed on the DC drive current, the optical power of the laser is an analog of the modulation waveform.

The laser current, $I(t)$, is represented by [20]

$$I(t) = I_b + I_m \cdot f(t) \quad (2-1)$$

where I_b is the DC bias current, I_m is the modulation current amplitude, and $f(t)$ is a function specifying the current modulation with minimum value of -1. As a simple example illustrating the theory, consider the case where $f(t)$ is a sinusoidal modulation. The function specifying the current modulation is now given as

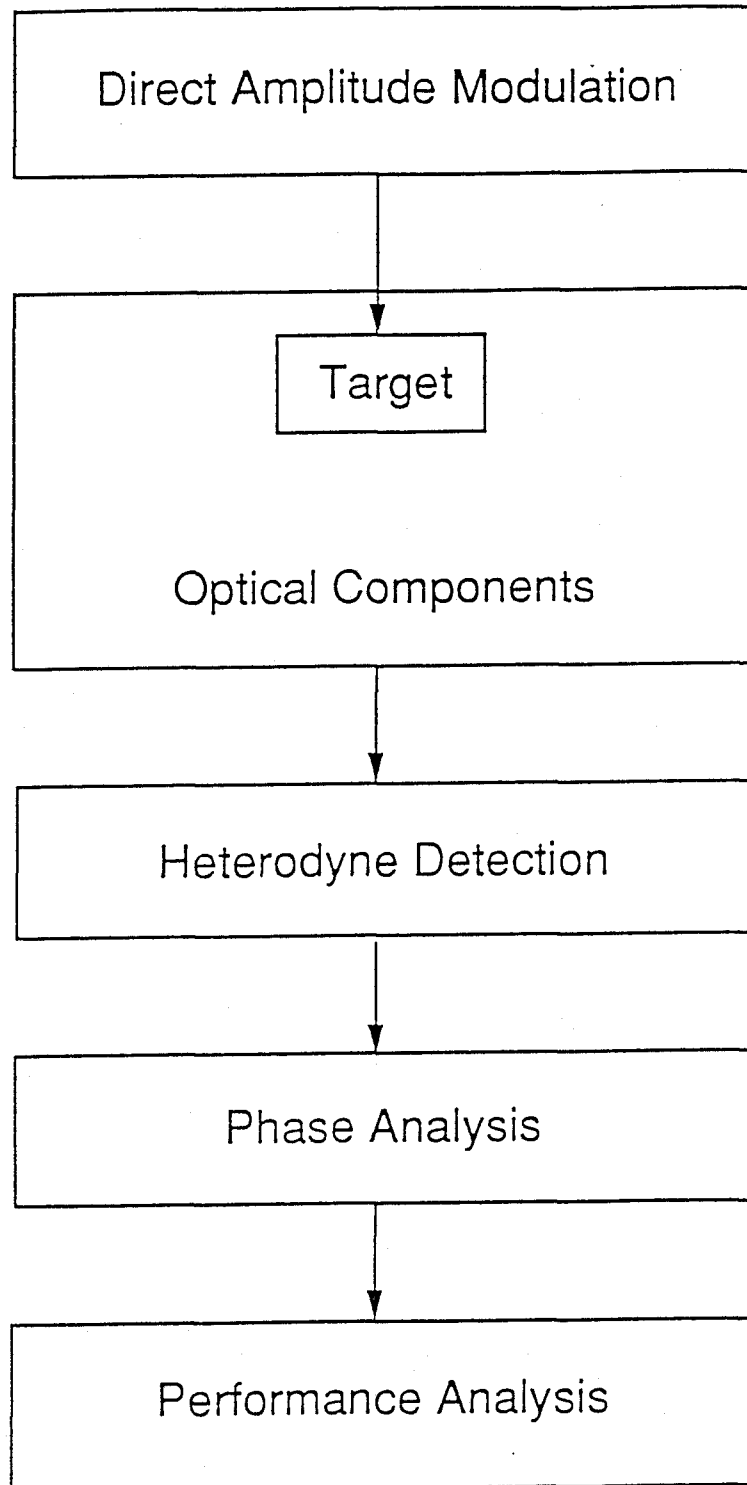


Fig. 2-1 Block diagram of the design process.

$$f(t) = \sin (2 \cdot \pi \cdot f_m \cdot t) \quad (2-2)$$

where f_m is the modulation frequency.

Assuming linear light/current characteristics of the diode laser, the output power becomes

$$P(t) = \eta \cdot \{I(t) - I_{th}\} = P_b + P_m \cdot \sin(2\pi f_m t) \quad (2-3)$$

where $\eta = (dP/dI)$ = the differential efficiency of the diode laser, and $P_b = \eta \cdot (I_b - I_{th})$ and $P_m = \eta \cdot I_m$ are the DC bias power and the modulated power, respectively. The variation of output power with input drive current is shown in Fig. 2-2.

Detailed physical treatments of direct modulation of semiconductor lasers have been given by Yariv [21] and by Welford and Alexander [22].

2.2 Heterodyne Detection and Beat Frequency

In this section, a beat frequency is described by a heterodyne detection from the directly amplitude modulated intensity (or power) of two laser beams. A schematic diagram of a heterodyne detection scheme is shown in Fig. 2-3.

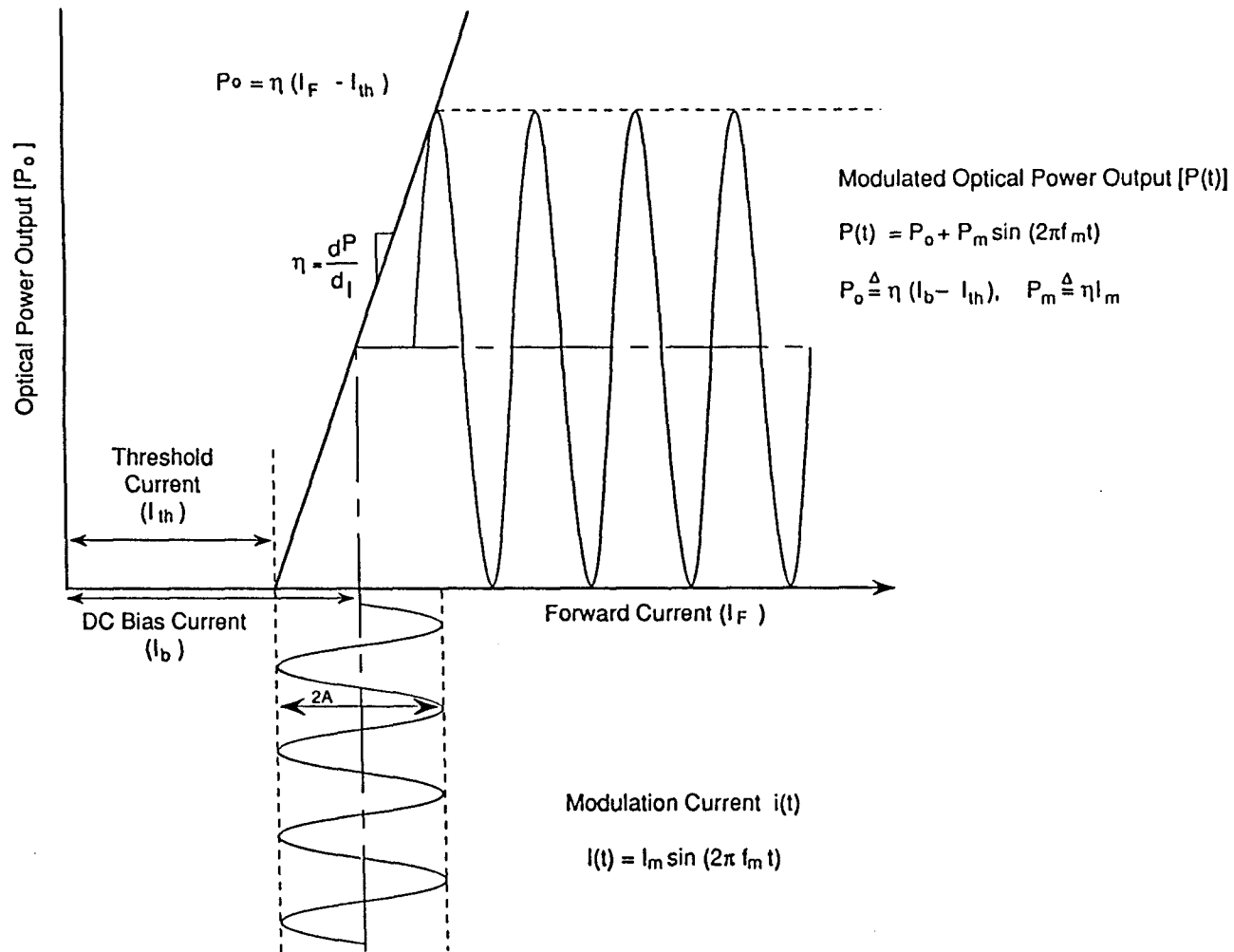


Fig. 2-2 Principle of direct amplitude modulation

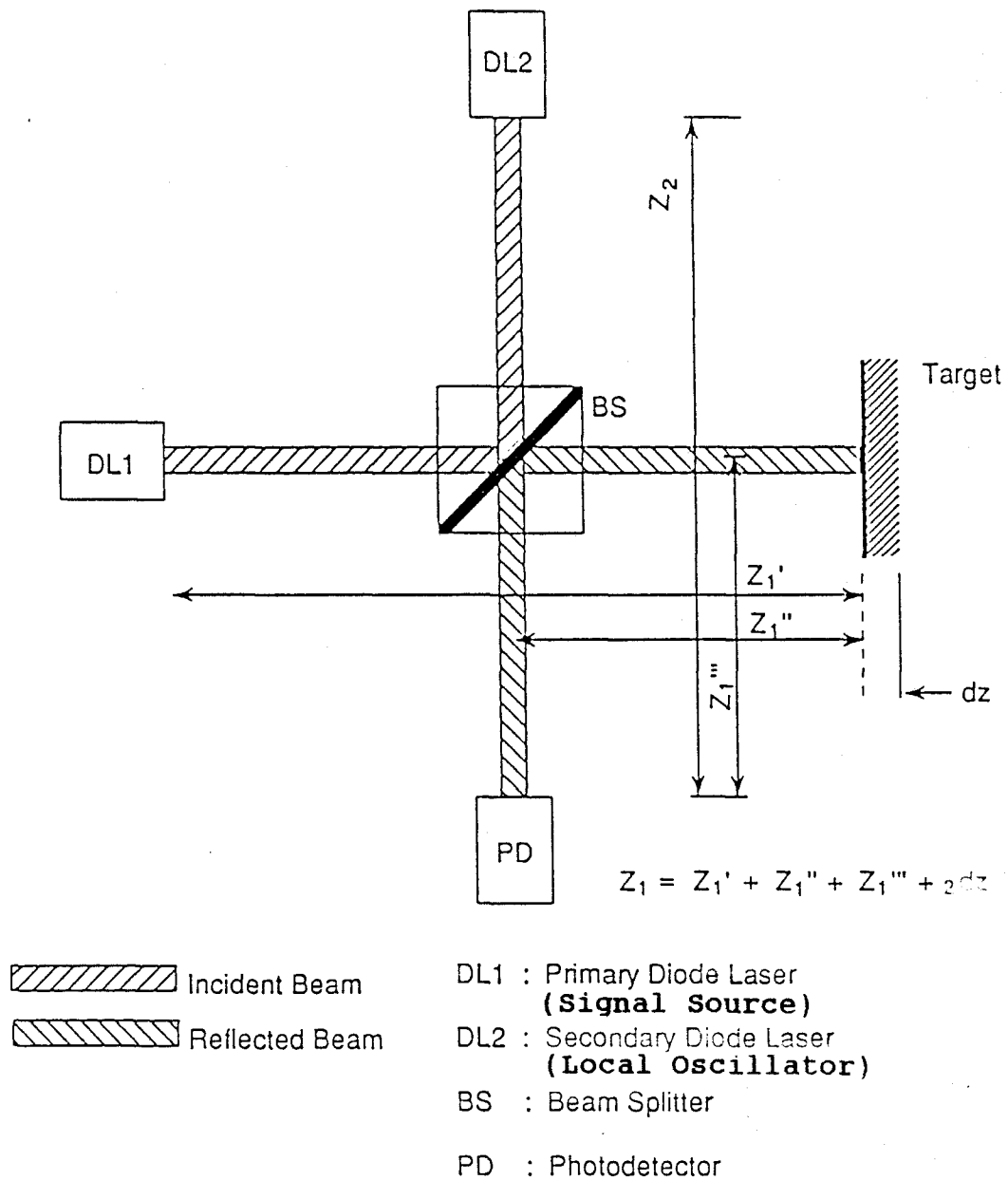


Fig. 2-3 Schematic diagram of a heterodyne detection system.

Assume that the two diode lasers have identical wavelengths and that the optical frequency, f_0 , is large compared to the modulation frequencies which are reasonably close together. Then the electric (or optical) fields of the two laser beams modulated at two frequencies, f_1 and f_2 , are written [3]

$$E_1(z_1, t) = A_1 \cdot \exp\{i(k_1 z_1 + w_1 \cdot t)\} \quad (2-4, a)$$

$$E_2(z_2, t) = A_2 \cdot \exp\{i(k_2 z_2 + w_2 \cdot t + \phi)\} \quad (2-4, b)$$

where A_1 and A_2 represent the modulated beam amplitudes of the two lasers, k_1 and k_2 are the propagation constants of the two lasers, $w_1 = 2 \pi f_1$, $w_2 = 2 \pi f_2$, and ϕ is the optical phase difference between the two beams at time $t = 0$.

The instantaneous incident optical intensity is [23]

$$I(z, t) = (1/2) \cdot \eta^{-1} \cdot |E(z, t)|^2 \quad (2-5)$$

where $\eta = (\mu_0 / \epsilon_0)^{1/2}$ is the characteristic impedance of free space (377 ohms).

If two laser beams are combined together on a detector with a square-law response, such as a solid state photodiode, the resulting effective intensity (I_{1+2}) is given by

$$\begin{aligned}
I_{1+2} &= (1/2) \cdot \eta^{-1} \cdot |A_1 \exp\{i(k_1 z_1 + w_1 t)\} + A_2 \exp\{i(k_2 z_2 + w_2 t + \phi)\}|^2 \\
&= (1/2) \cdot \eta^{-1} \cdot [\{ A_1 \cos(k_1 z_1 + w_1 t) + A_2 \cos(k_2 z_2 + w_2 t + \phi) \}^2 \\
&\quad + \{ A_1 \sin(k_1 z_1 + w_1 t) + A_2 \sin(k_2 z_2 + w_2 t + \phi) \}^2] \\
&= (1/2) \cdot \eta^{-1} [A_1^2 + A_2^2 + 2A_1 A_2 \cos\{(k_1 z_1 - k_2 z_2) + (w_1 - w_2)t + \phi\}] \\
&\quad (2-6)
\end{aligned}$$

As was stated earlier, since f_1 and f_2 are close together, $k_m \approx k_1 \approx k_2$ and Eqn. (2-6) becomes

$$I_{1+2}(t) = I_0 + I_m \cos\{2\pi \cdot |f_1 - f_2| \cdot t + k_m(z_1 - z_2) + \phi\} \quad (2-7)$$

where the constant terms are $I_0 = (1/2) \cdot \eta^{-1} \cdot (A_1^2 + A_2^2)$ and $I_m = \eta^{-1} \cdot A_1 \cdot A_2$.

For fixed positions, that is, where z_1 and z_2 are fixed, the light intensity viewed by a photodetector contains a time-varying component of $|f_1 - f_2|$ which is the heterodyne signal at the beat frequency, $f_b = |f_1 - f_2|$.

In Eqn. (2-7), assuming that z_1 is the distance between the signal laser (DL1) and the detector (PD) (see Fig. 2-3), and assuming that z_2 is a constant reference distance from the local oscillator laser (DL2), z_1 becomes $z_{10} + 2 \cdot dz$, where z_{10} is the z_1 distance at the target "zero" position and dz is the target displacement from "zero". For example, setting $z_{10} = z_2$ and $\phi = 0$, or $z_{10} \cdot k_m + \phi = 0$, Eqn. (2-7) is rewritten as

$$I_{1+2}(t) = I_0 + I_m \cdot \cos(2 \cdot \pi \cdot f_b \cdot t + d\phi) \quad (2-8)$$

where

$$d\phi = k_m \cdot (2 \cdot dz) = (4 \cdot \pi \cdot c / f_m) \cdot dz \quad (2-9)$$

which is the phase shift caused by the target displacement, dz . Equation (2-9) shows that the phase shift $d\phi$ is linearly dependent on dz . Therefore, it is now clear that the phase difference can be used as a measure of the range.

As was shown in Eqn. (2-9), any small net displacement measurement, dz , can easily be determined in terms of the phase shift

$$dz = (c / 4 \cdot \pi \cdot f_m) \cdot d\phi \quad (2-10)$$

However, the measurement of the phase shift, $d\phi$, is unambiguous only if $d\phi$ does not exceed 2π radians. Substituting $d\phi = 2\pi$ into Eqn. (2-10) gives the maximum unambiguous range of displacement measurements. A plot of the maximum unambiguous range as a function of modulation frequency is shown in Fig. 2-4.

MAXIMUM UNAMBIGUOUS RANGE VS. FREQUENCY

$$R(\text{max.unamb.}) = c / (2 f_m)$$

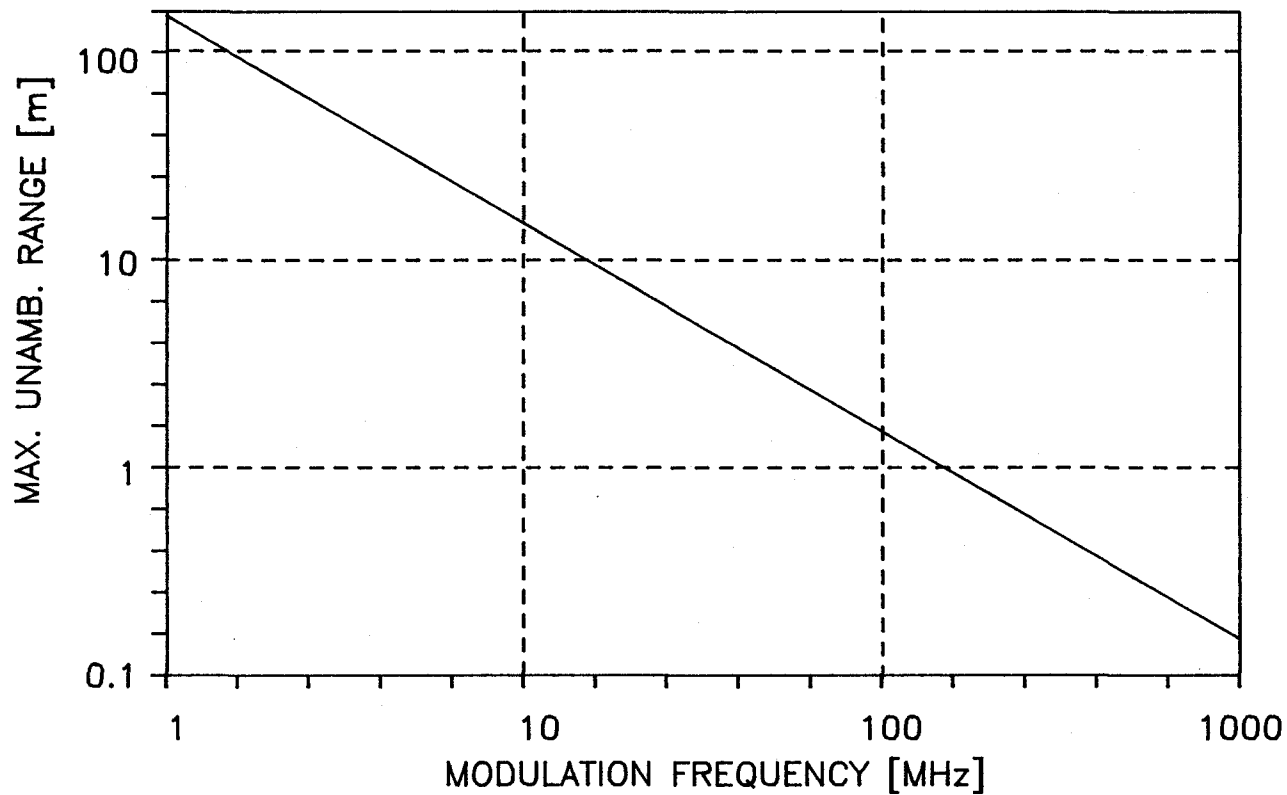


Fig. 2-4 Plot of maximum unambiguous range versus modulation frequency.

2.3 Laser Ranging

The current produced by a photodetector of area A in response to the optical power incident on the photodetector is [23], [24]

$$i(t) = \left(\eta \cdot q / h \cdot f_0 \right) \int_A I_{1+2}(t) dA \quad (2-11)$$

where η is the photodetector quantum efficiency, q is the electron charge ($1.60218E-19$ [C]), h is Plank's constant ($6.62617E-34$ [J·s]), and f_0 is the optical frequency of the diode laser ($f_0 = c / \lambda$). Assuming that the photodetector area A is sufficiently large to intercept all of the light, and combining Eqns. (2-6) and (2-11), the total photodetector current as a function of the signal power (P_S) and the local oscillator power (P_{LO}) is rewritten

$$i(t) = \left(\eta q / h f_0 \right) \left[P_{LO} + P_S + 2(P_{LO} \cdot P_S)^{\frac{1}{2}} \cdot \cos(2\pi f_D t + d\Phi) \right] \quad (2-12)$$

Equation (2-12) is the basic heterodyne equation with its last term referred to as the heterodyne term. The heterodyne signal is a small modulation superimposed on top of the DC current level. The total DC current through the photodetector contributes shot noise at the beat frequency due to its quantum fluctuations. However,

since the beat frequency is predetermined, the heterodyne signal can be electronically filtered out in order to reduce the noise to any (non-zero) level desired. If the AC current from the photodetector drives a load resistance of R_L , the heterodyne signal power, P_H , is

$$P_H = 2 \cdot (\eta \cdot q / h \cdot f_o)^2 \cdot P_{LO} \cdot P_S \cdot R_L \quad (2-13)$$

Equation (2-13) shows that the heterodyne signal from the photodetector is directly proportional to the signal power and to the local oscillator power.

The noise in heterodyne detection is dominated by the shot noise or quantum fluctuations of the local oscillator beam for sufficiently high local oscillator power and for sufficiently high modulation frequency [25], [26]. For the normal case in which $P_{LO} \gg P_S$, the shot noise power, P_N , from the photodetector at the beat frequency is

$$P_N = 2 \cdot q \cdot (\eta \cdot q / h \cdot f_o) \cdot P_S \cdot BW \cdot R_L \quad (2-14)$$

where BW is the detection bandwidth.

The signal-to-noise ratio, S/N , of the heterodyne signal is determined from Eqns. (2-13) and (2-14),

$$S/N = (\eta \cdot P_S) / (h \cdot f_o \cdot BW) \quad (2-15)$$

Combining Eqns. (2-10) and (2-15), the displacement measurement accuracy is finally determined to be

$$dz_{\text{rms}} = c / [4 \cdot \pi \cdot f_m \sqrt{ 2 \cdot (\eta \cdot P_s) / (h \cdot f_o \cdot BW) }] \quad (2-16)$$

Theoretical results of the measurement accuracy based on Eqn. (2-16) are shown in Fig. 2-5 assuming a quantum efficiency of 0.48 and a BW of 100 Hz. These results indicate that a displacement measurement accuracy of less than 13 μm is found at the heterodyne signal power level of over 1 μW in the modulation frequency range of 10 MHz to 1 GHz. The experimental setup and its results will be discussed in the following chapter.

RESOLUTION VS. HETERODYNE SIGNAL POWER

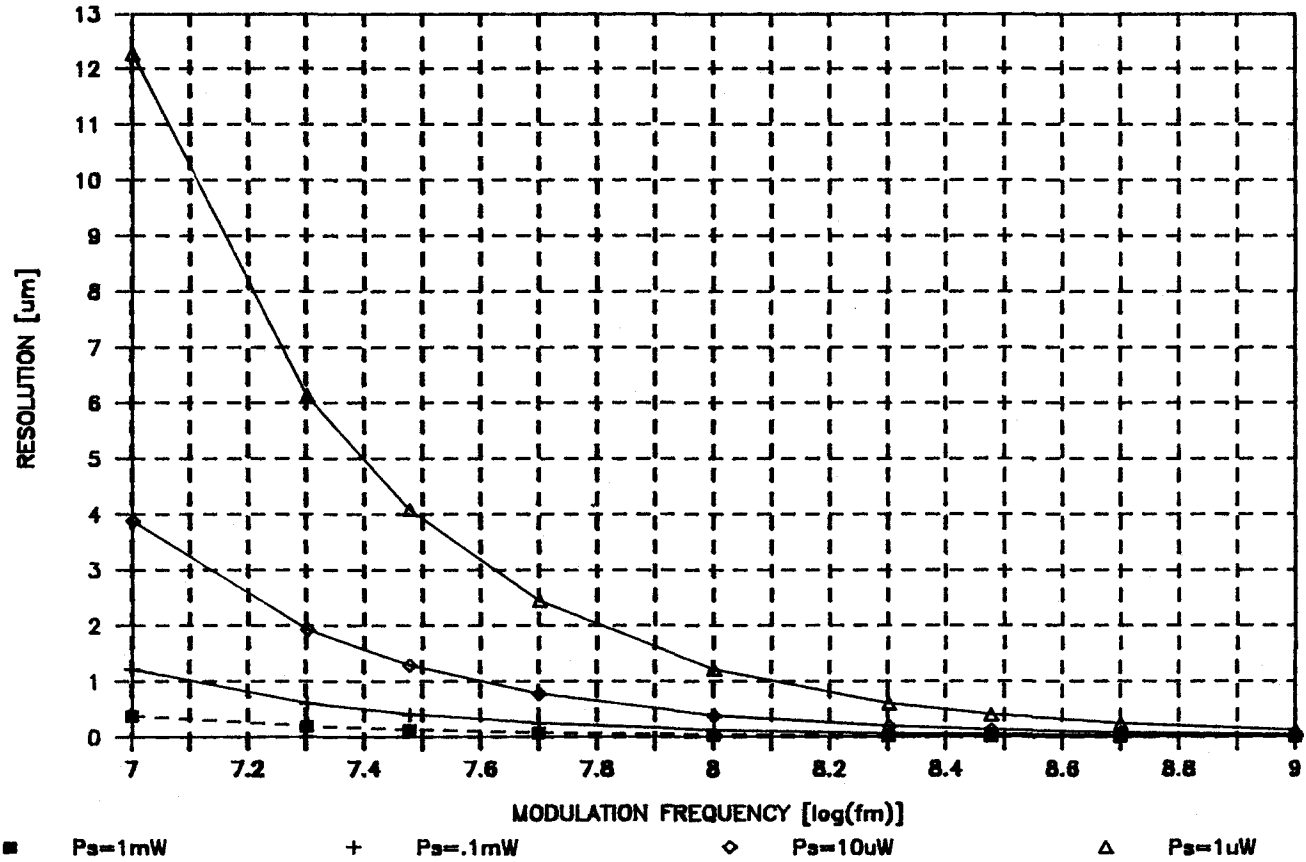


Fig. 2-5 Plot of displacement accuracy as a function of heterodyne signal power level (BW = 100 Hz).

3. EXPERIMENTS AND RESULTS

Figure 3-1 shows a schematic diagram of a dual-frequency diode laser displacement sensor used as a ranging measurement system. Various critical components and overall performance of the sensor system will be discussed in subsequent sections:

1. Direct Amplitude Modulation of Diode Lasers
2. System Alignment
3. Optical Heterodyne Detection
4. Performance Analysis

3.1 Direct Amplitude Modulation of Diode Lasers

3.1.1. Experiment

The local oscillator laser was a commercial Ortel, Inc. with a 6 GHz modulation bandwidth. It has a DC bias supply and a separate modulation input directly to the laser head through an SMA connector. This laser as well as two bias tees were provided by Lucidyne Technologies, Inc. of Corvallis, Oregon who also provided partial financial support.

A second drive circuit for a commercial compact disc (CD) semiconductor diode laser was designed in order to produce a directly amplitude modulated laser beam for the

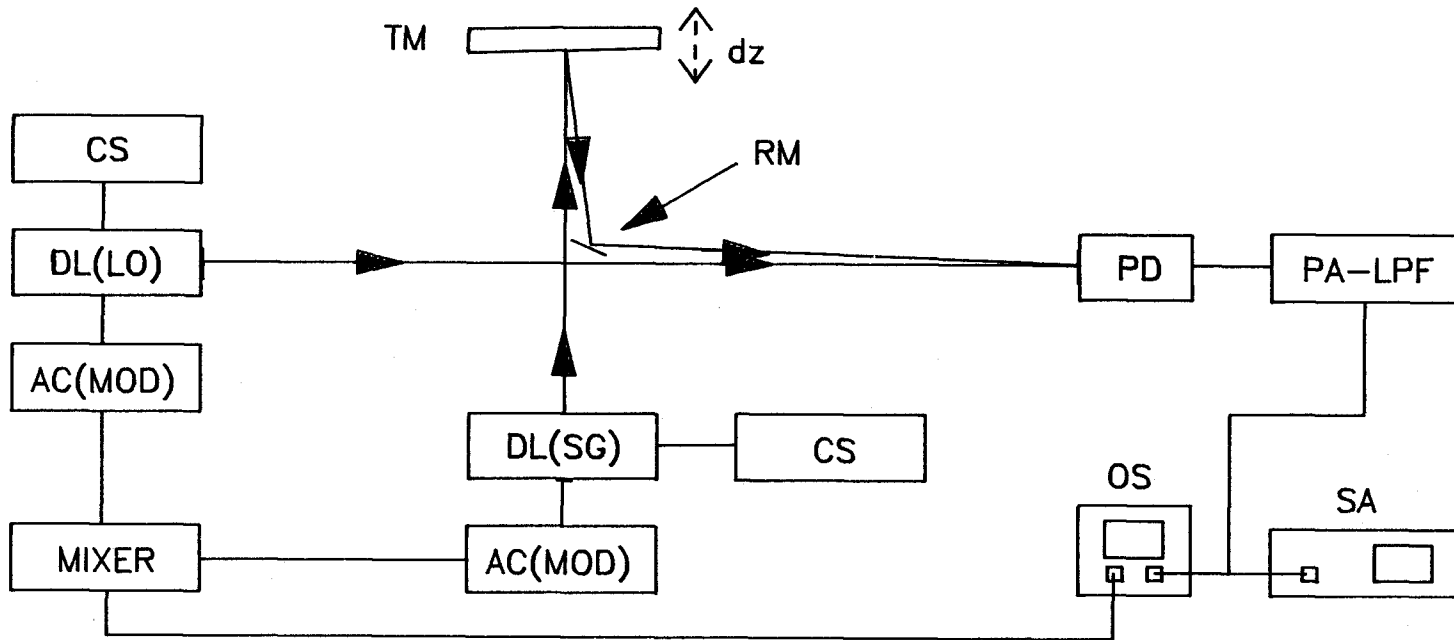


Fig. 3-1 Schematic diagram of experimental setup of a dual-frequency diode laser displacement sensor.

CS: Current Source (DL: Diode Laser, LO: Local Oscillator, SG: Signal),
 MIXER: frequency MIXER, MOD: Synthesized signal generator for MODulation,
 OS: OscilloScope, PA-LPF: Pre-Amplified Low Pass Filter, PD: PhotoDetector,
 RM: Relay Mirror, SA: Spectrum Analyzer, TM: Target Mirror, dz: displacement.

signal source. A single mode GaAlAs laser diode (Sharp LTO 22 MC0) with an emitting wavelength of 780 nm was used [27]. The manufacture claims a 1 GHz modulation bandwidth.

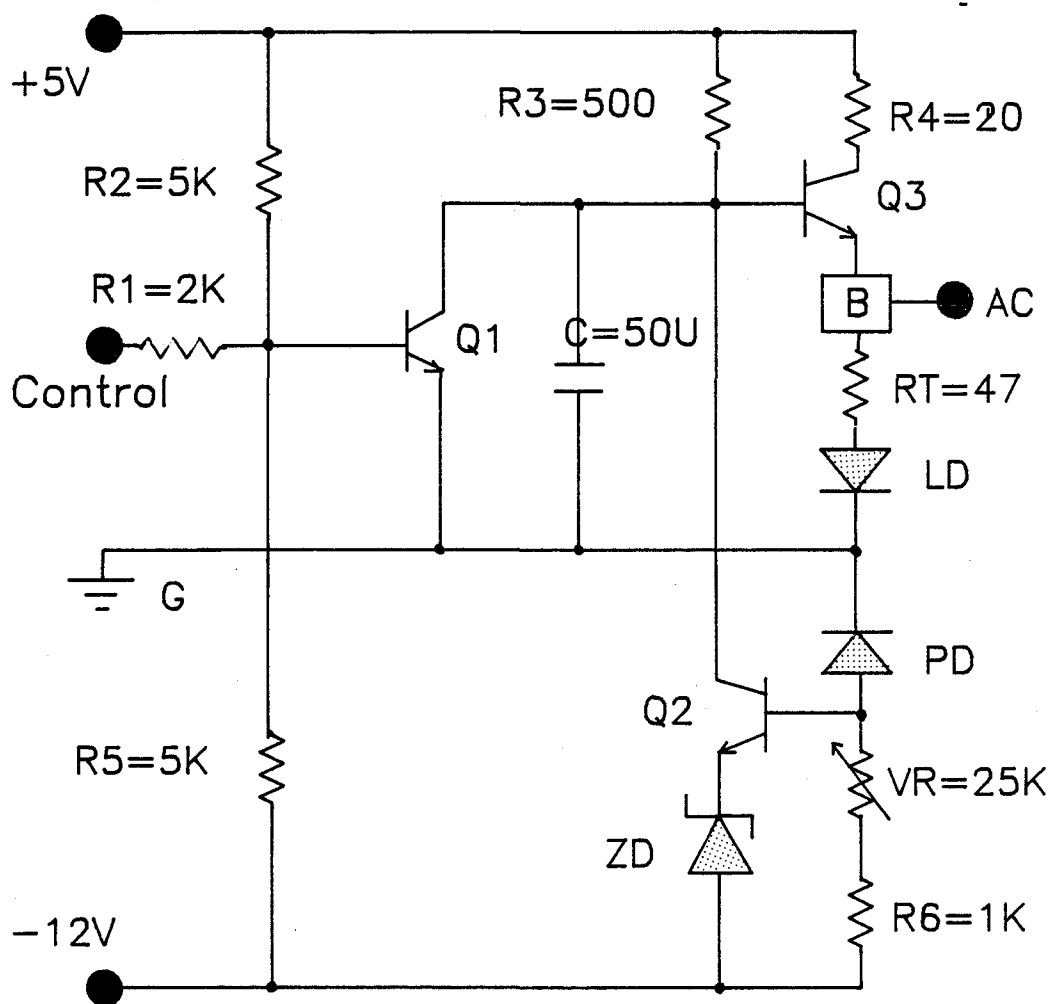
As shown in Fig. 3-2, a drive circuit was designed with an automatic power control function that acts as a feedback loop from the output of the monitor photodiode to the input of the laser diode. This control circuit was used to maintain constant power output in an environment where temperature may vary and cause changes in the power output of the laser diode. The circuit also features a slow start characteristic to eliminate any electrical current (power) surge.

Employing a bias tee connector between the drive circuit and a diode laser, a synthesized signal generator (Fluke 6061A 10 kHz - 1050 MHz) was input as the modulation current source.

To achieve a small, nearly straight beam from the diode laser, a collimating lens (Fujinon LSR / F11A f=4.5 mm) was mounted on an XYZ stage (Line Tool Co. Model A RH). It was possible to achieve a nearly parallel beam containing almost all of the total laser output.

3.1.2. Results

Using an optical power meter (UDT Model#247 40xOpto-Meter), the output power versus forward current was measured to find a proper DC bias current for amplitude



Q1, Q2, & Q3 = Archer 276-2009

ZD = Archer 276-561

B = Commercial Bias Tee

Fig. 3-2 Drive circuit for direct amplitude modulation of CD laser diode.

modulation. It was also necessary to calibrate the monitor current of the photodetector in the laser package.

The diode laser characteristics are plotted in Fig. 3-3 (a) and (b). The desired output power level of 3 mW corresponded to a DC forward current of 60 mA, and the differential efficiency, η , of the diode laser was found to be $\eta = .25 \text{ mW/mA}$. As a result, the amplitude of AC modulation current was set at 10.8 mA which gave a modulation depth of about 90 %. Because of the high speed modulation, voltage controlled source instead of the current controlled source served as the modulation input source.

Typical waveforms of the directly amplitude modulated signal are shown in Fig. 3-4. In Fig. 3-4 (a), the driving conditions were $I_F = 59.3 \text{ mA}$ and V_{AC} (peak-to-peak) = 20 mV at $f_m = 500 \text{ MHz}$. In Fig. 3-4 (b), the conditions were $I_F = 54.8 \text{ mA}$ and $V_{AC} = 50 \text{ mV}$ at $f_m = 50 \text{ kHz}$. The large input current swing in Fig. 3-4 (b) caused the drive current to fall below the threshold level ($I_{th} = 44 \text{ mA}$) which shows a cut-off region in the modulation output signal. To achieve large modulation without introducing higher order frequency components in the flattened cut-off region, the modulation current was kept above the threshold level by 5 mA.

FORWARD CURRENT VS. OUTPUT POWER

(SHARP LTO 22 MCO LASER DIODE)

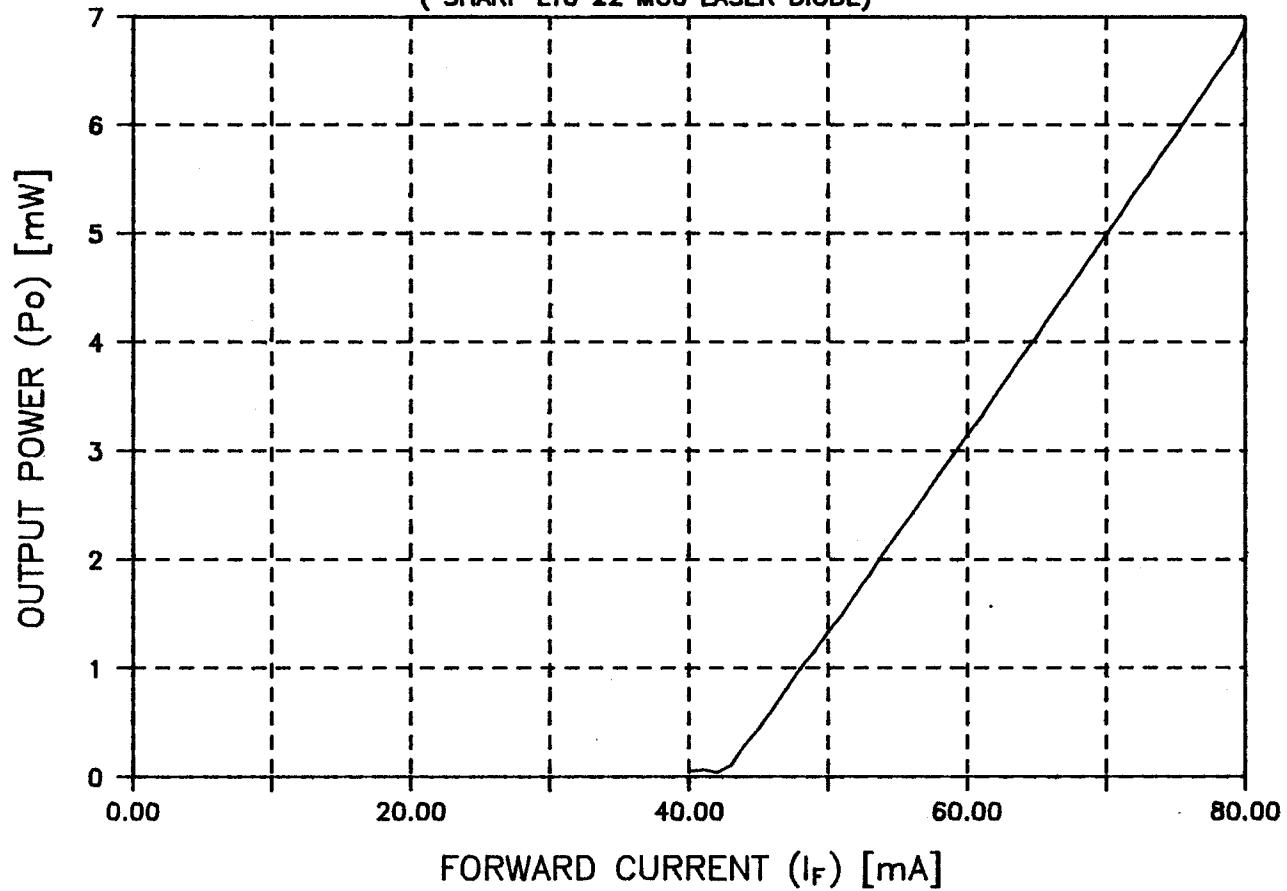


Fig. 3-3 (a) Plot of optical power versus forward current.

MONITOR CURRENT VS. OUTPUT POWER

(SHARP LTO 22 MCO LASER DIODE)

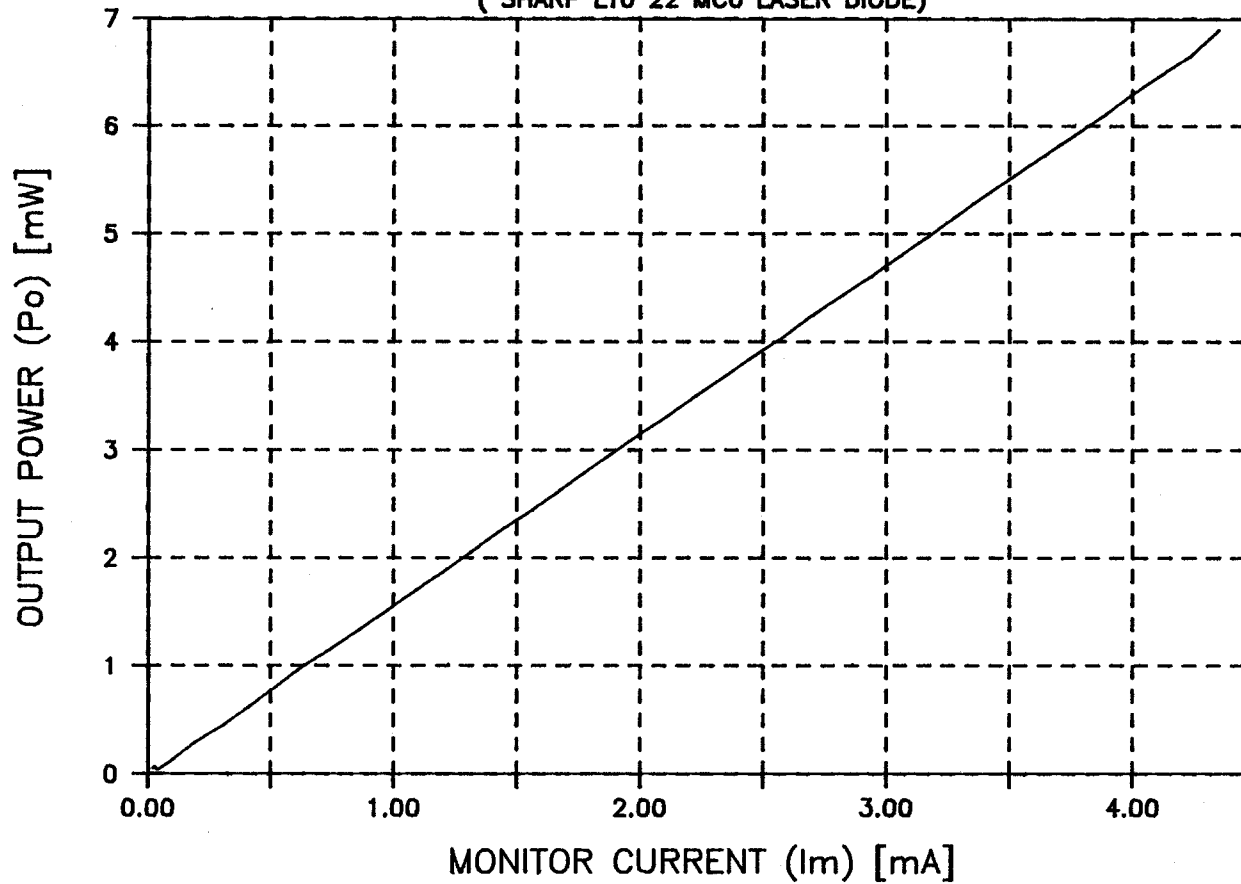
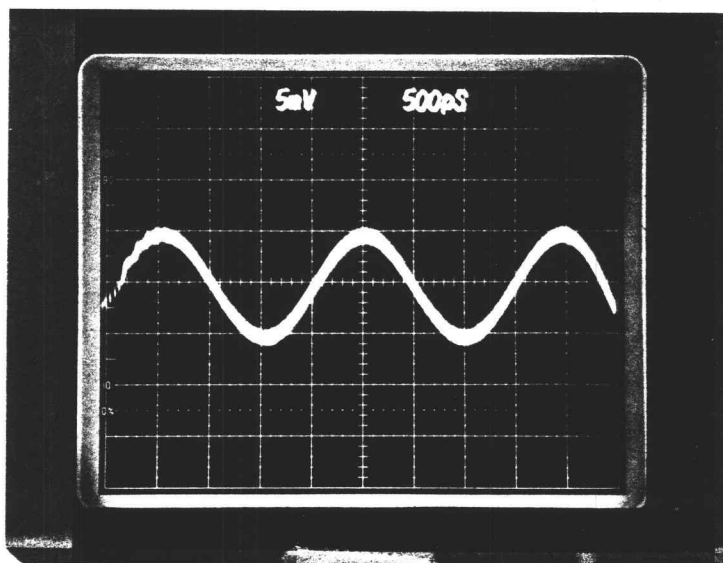
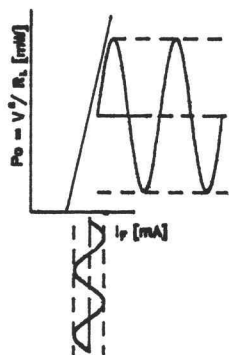
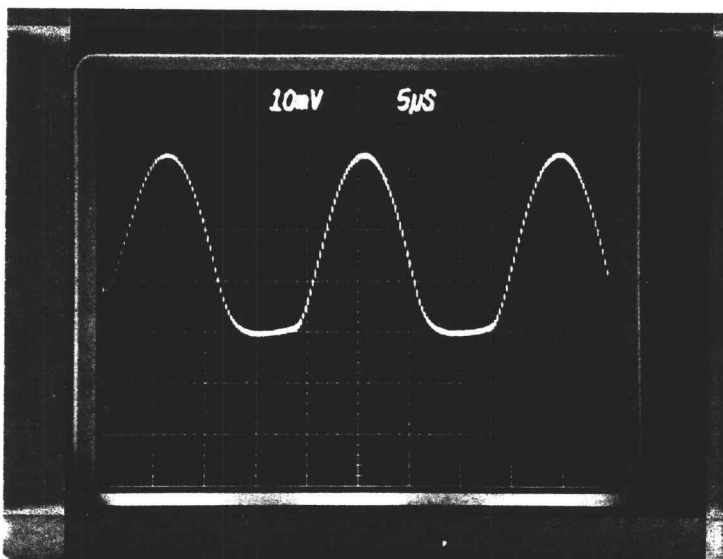
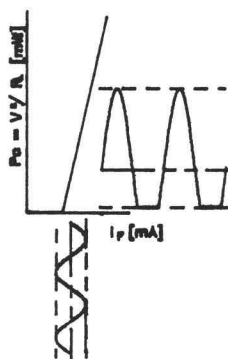


Fig. 3-3 (b) Plot of optical power versus monitor current.



(a)



(b)

Fig. 3-4 Monitored oscilloscope traces of direct amplitude modulation at $f_m = 500$ MHz.
 (a) shows a typical amplitude modulation.
 (b) shows a cut-off modulation due to insufficient DC bias level.

3.2 System Alignment

As shown in Fig. 3-1, the local oscillator laser beam from (DL2) was collimated and directly focused onto the photodetector (IRI 8016, whose surface diameter is measured as 1 mm). The collimated signal laser (DL1) was transmitted toward the target mirror (a reflectivity of 90% was assumed), reflected to the gold-coated relay mirror ($R = 90\%$ at the wavelength of 780 nm [28]), and then directed onto the photodetector. The target mirror was mounted on a sliding rail with a built-in scale, to measure target displacements.

3.3 Optical Heterodyne Detection

3.3.1. Experiment

A simple circuit for the operation of a photodetector and amplification of its output is shown in Fig. 3-5. The output was connected to either an oscilloscope (Tektronix 7904 for high frequency observations of signal and local oscillator output waveforms, Tektronix 2230 100MHz Digital Storage Oscilloscope for low frequency observations of heterodyne signal waveforms and their phase shifts) or a spectrum analyzer (Tektronix 2756P Programmable Spectrum Analyzer for frequency responses and power levels). The circuit

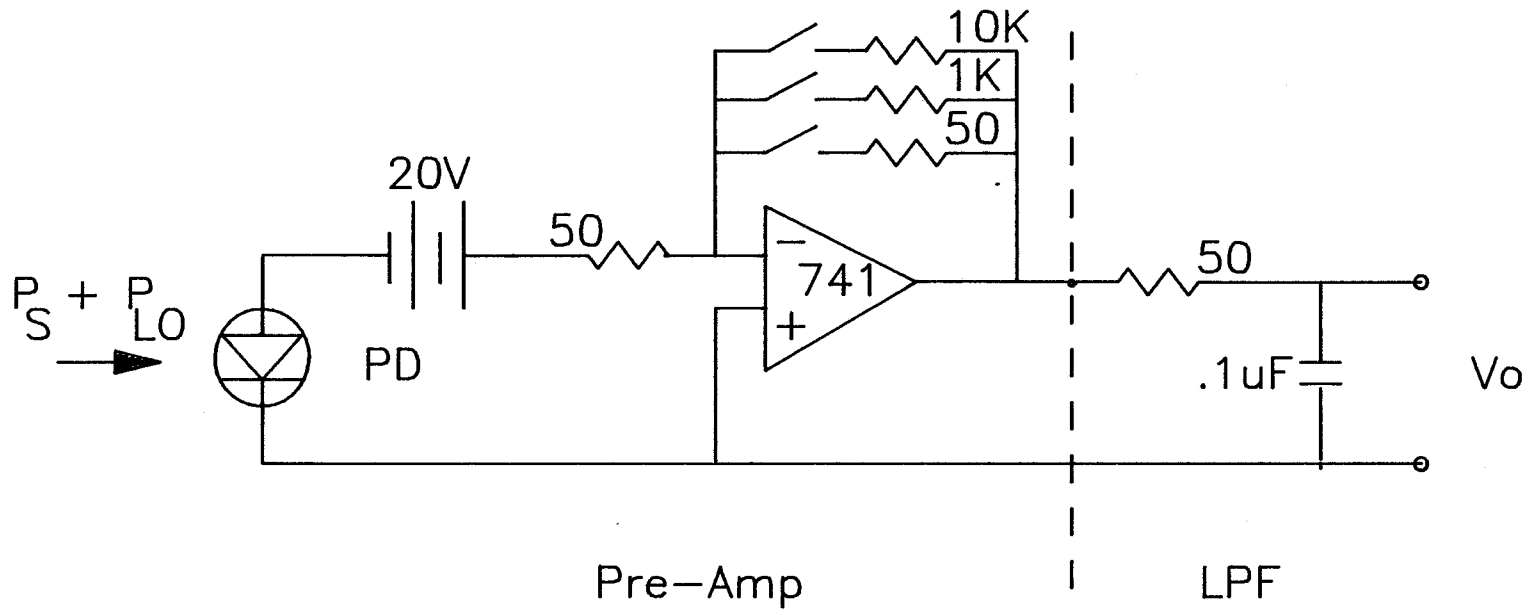


Fig. 3-5 Optical heterodyne detection circuit.

Pre-Amp indicates the pre-amplification stage, and LPF the Low Pass Filter.

shown in Fig. 3-5 consists of two sub-stages: the pre-amplification stage which amplifies the mixed signal level and the low pass stage which filters out the heterodyne signal frequency after both the signal and local oscillator beams have been optically coupled and mixed at the photodetector surface.

The beat signal, whose frequency was equal to the difference of the signal and local oscillator frequencies, was simply extracted from the photocurrent passing through the low pass filter circuit tuned to the beat frequency. On an oscilloscope, the phase of the beat signal at each target mirror position was detected immediately by comparing it with an electronic reference signal obtained by means of a frequency mixer (HP 10514A Mixer S#833) into which the signal and local oscillator frequencies were fed. Using a spectrum analyzer the power level of the beat signal was checked and measured.

3.3.2. Results

The collimated signal and local oscillator laser beams, whose DC biased optical powers were set at 3 mW by monitoring DC bias current sources, were modulated at frequencies of 100.00 and 100.01 MHz, respectively. Therefore, the beat signal generated had a carrier frequency of 10 KHz. The beat signal obtained was stable when compared with the electronic reference signal from the mixer.

An example is shown in Fig. 3-6 (a) and (b) where a spectrum analyzer has been used. Figure 3-6 (a) shows the signal and local oscillator detected. Figure 3-6 (b) shows the beat signal, which had been already amplified by a differential amplifier (Tektronix AM502, Gain = 20 k, HF-3dB = .1 MHz, LF-3dB = 10 kHz, - channel was grounded) and filtered through a low pass at $f_c = 16$ kHz.

The photographs shown in Fig. 3-7 (a) and (b) were taken with a scope camera (Tektronix C-59A Oscilloscope Camera). Figure 3-7 (a) shows the 10 kHz beat signal from the photodiode without amplifying or filtering. Figure 3-7 (b) shows the clustered signal and the thick signal which denote the traces of the beat and the electronic reference signals at 50 kHz, respectively. These results indicate that the laser heterodyne method is successfully available in the displacement measurement.

3.4 Performance Analysis

3.4.1. Experiment

With all of the previous experiments and results in place, it was possible to make an estimate of the performance of a dual-frequency diode laser displacement sensor. Displacement measurements were made by moving the target mirror on the optical rail to increase or decrease the optical path length. From the electrical reference

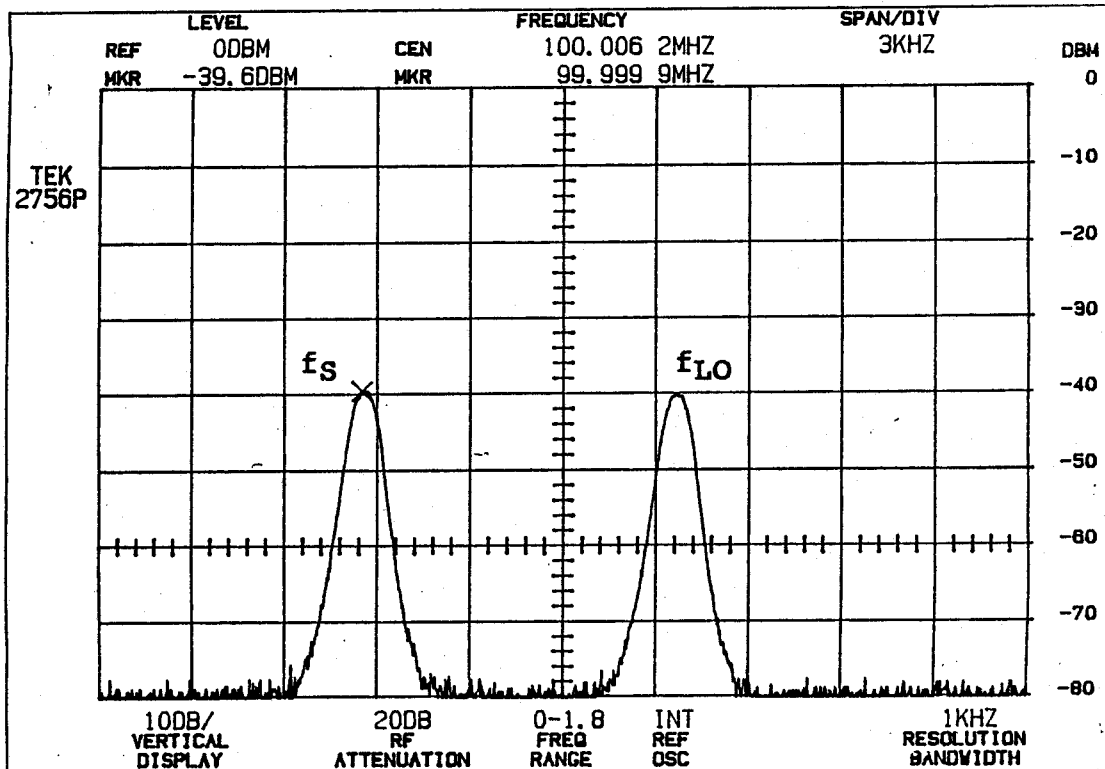


Fig. 3-6 (a) Optical heterodyne detection of the signal and local oscillator light sources by a spectrum analyzer.
($f_s = 100.00$ MHz and $f_{LO} = 100.01$ MHz)

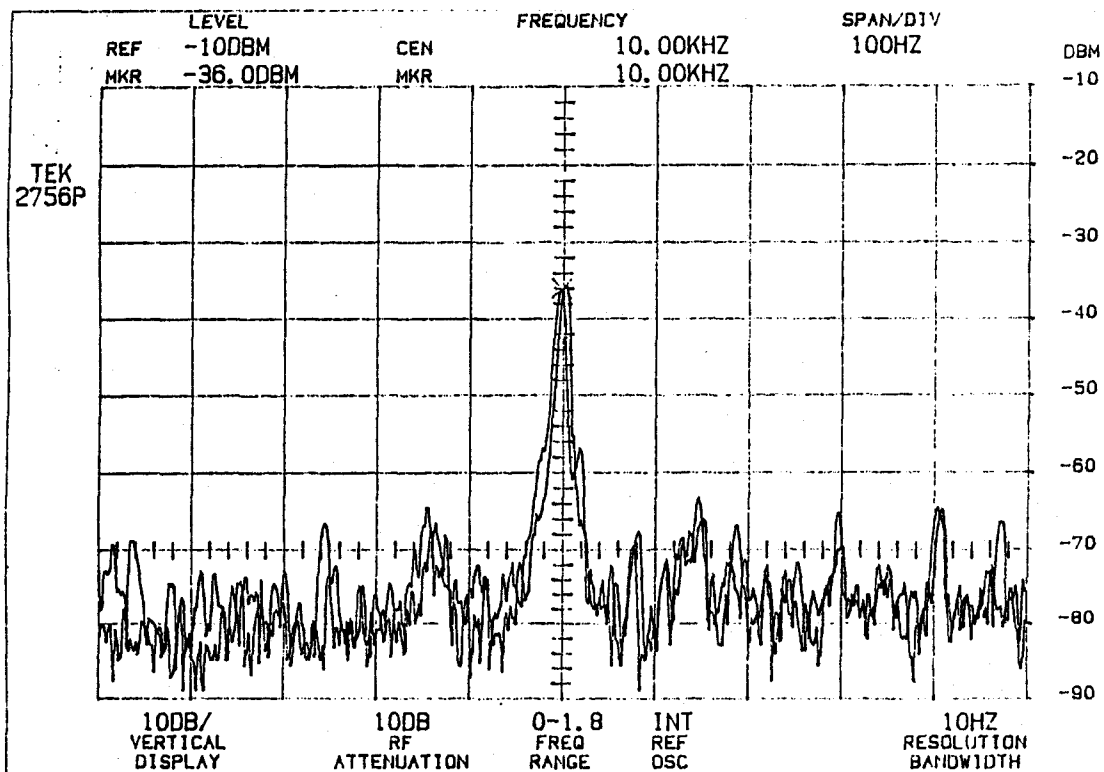


Fig. 3-6 (b) Optical heterodyne detection of a beat signal ($f_b = 10$ KHz)
Two scans overlapped to show repeatability.

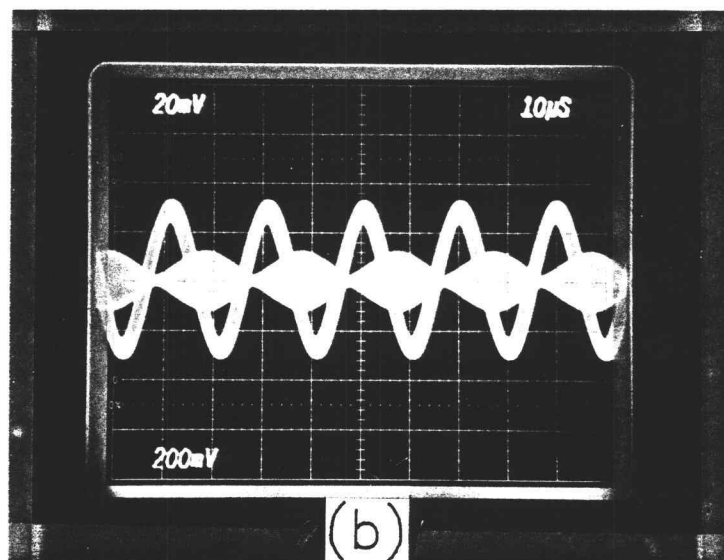
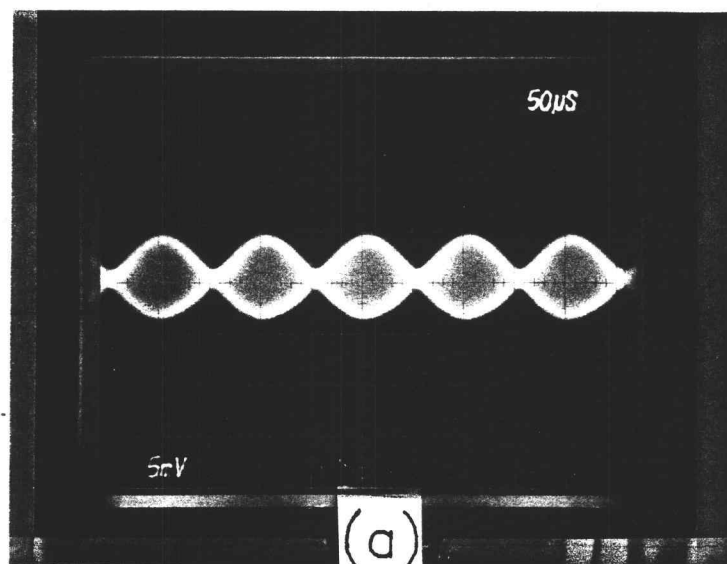


Fig. 3-7 Optical heterodyne detection output waveforms on an oscilloscope.

signal and the beat signal, a phase difference corresponding to displacement was measured. At each of the target mirror positions, the phase shift was measured on the oscilloscope, and the beat signal and noise power level were measured using the spectrum analyzer.

Five different modulation frequencies (10 MHz, 50 MHz, 100 MHz, 200 MHz, and 300 MHz) were used at the initial setting; then the distance was increased by 10.00 mm increments until the phase shift of the beat signal (10 kHz) was about 360 degrees.

3.4.2. Results

In Fig. 3-8 (a), the upper photograph shows the "zero" phase difference of the initial position of the target mirror. The electrical reference ($f_{LO} = 100.01$ MHz, $f_S = 100$ MHz) from the mixer (upper trace) and the beat signal detected from the photodetector (lower trace) are 180 degree out of phase - it doesn't matter as long as it fixes the reference relationship. The lower photograph shows phase difference after the target mirror had been moved 37.5 cm to produce a $d\Phi$ of 90 degrees.

In Fig. 3-8 (b), the upper photograph ($f_{LO} = 10.01$ MHz, $f_S = 10$ MHz) shows a reference "zero" phase difference of -14 degrees, while the lower photograph shows a +28 degree phase difference at a displacement of 180 cm, which indicates a net phase shift of 42 degrees

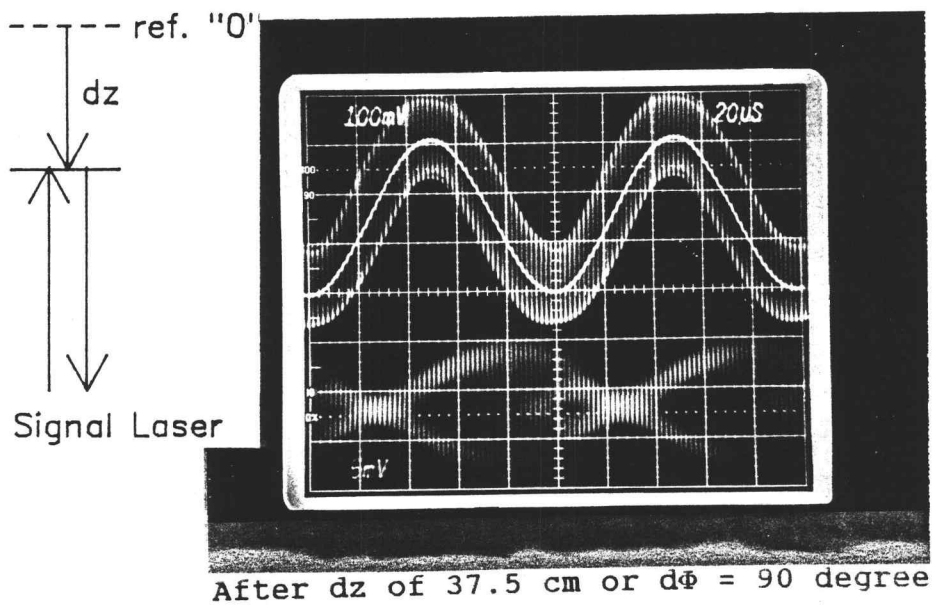
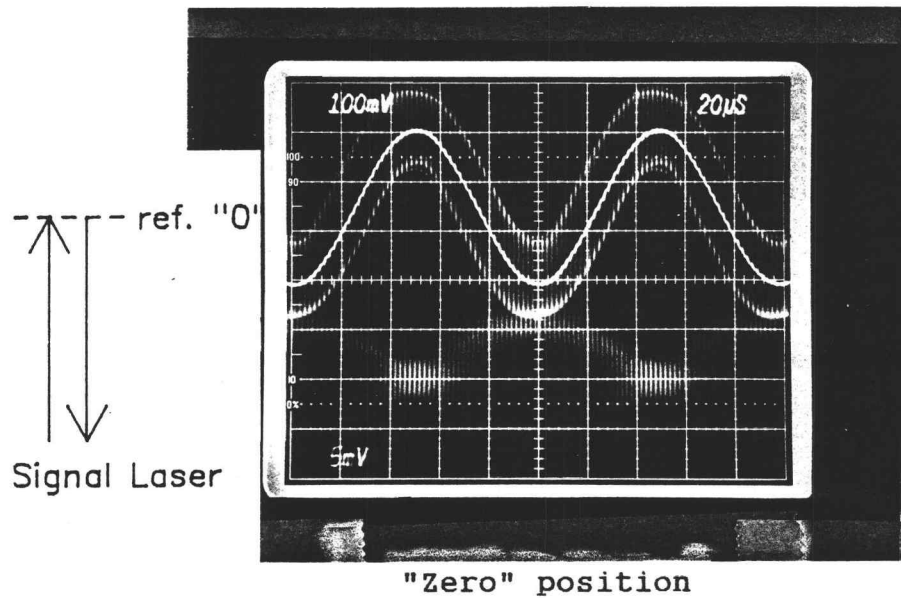


Fig. 3-8 (a) Monitored oscilloscope traces. ($f_S = 100.00$ MHz, $f_{LO} = 100.01$ MHz, and $dz = 37.5$ cm)

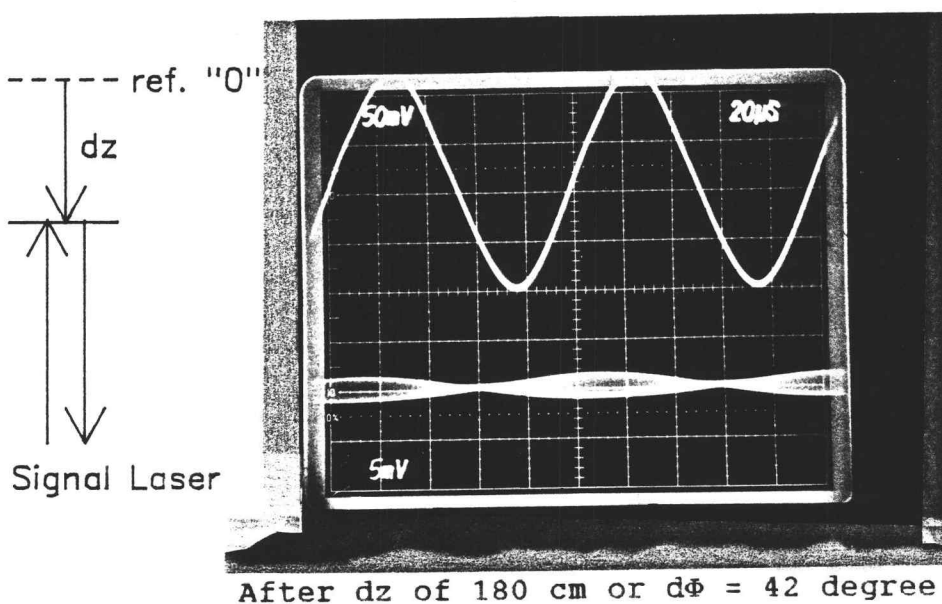
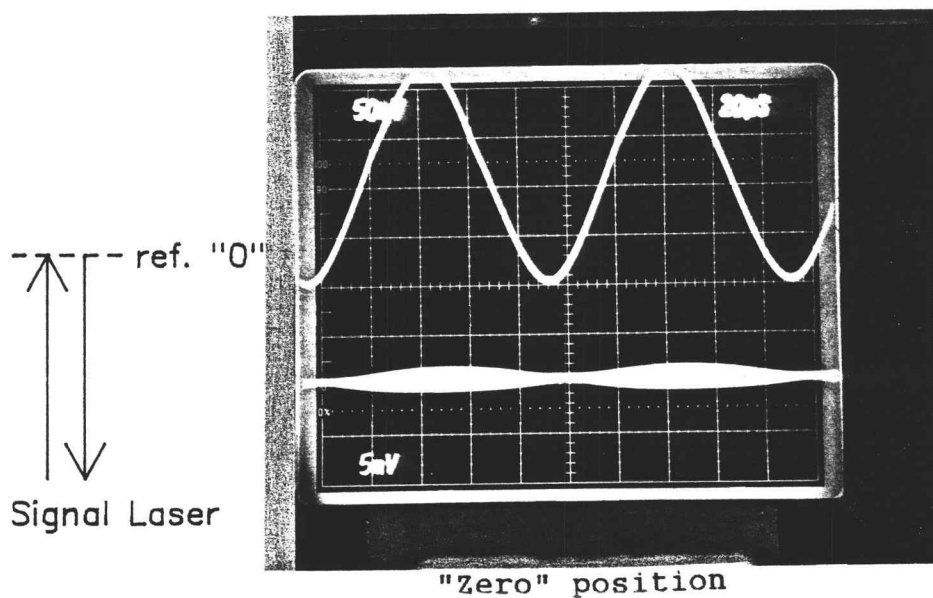


Fig. 3-8 (b) Monitored oscilloscope traces. ($f_S = 10.00$ MHz, $f_{LO} = 10.01$ MHz, and $dz = 180$ cm)

for that displacement. The calculated value is 43.2 degrees.

Figure 3-9 shows the measured phase shifts at the tested frequencies as a function of the relative displacement, which is the distance difference between the initial position of the target mirror and its position after it is moved. In order to see a phase shift of 360 degrees in the beat signal at a modulation frequency of 10 MHz, the required displacement is 15 m. Due to the difficulty of making long optical paths in our laboratory the maximum tested displacement was 350 cm. Figure 3-9 shows that the phase shift is linear with optical path difference (i.e., the displacement) in good agreement with theory.

PHASE SHIFT VS. MODULATION FREQUENCY

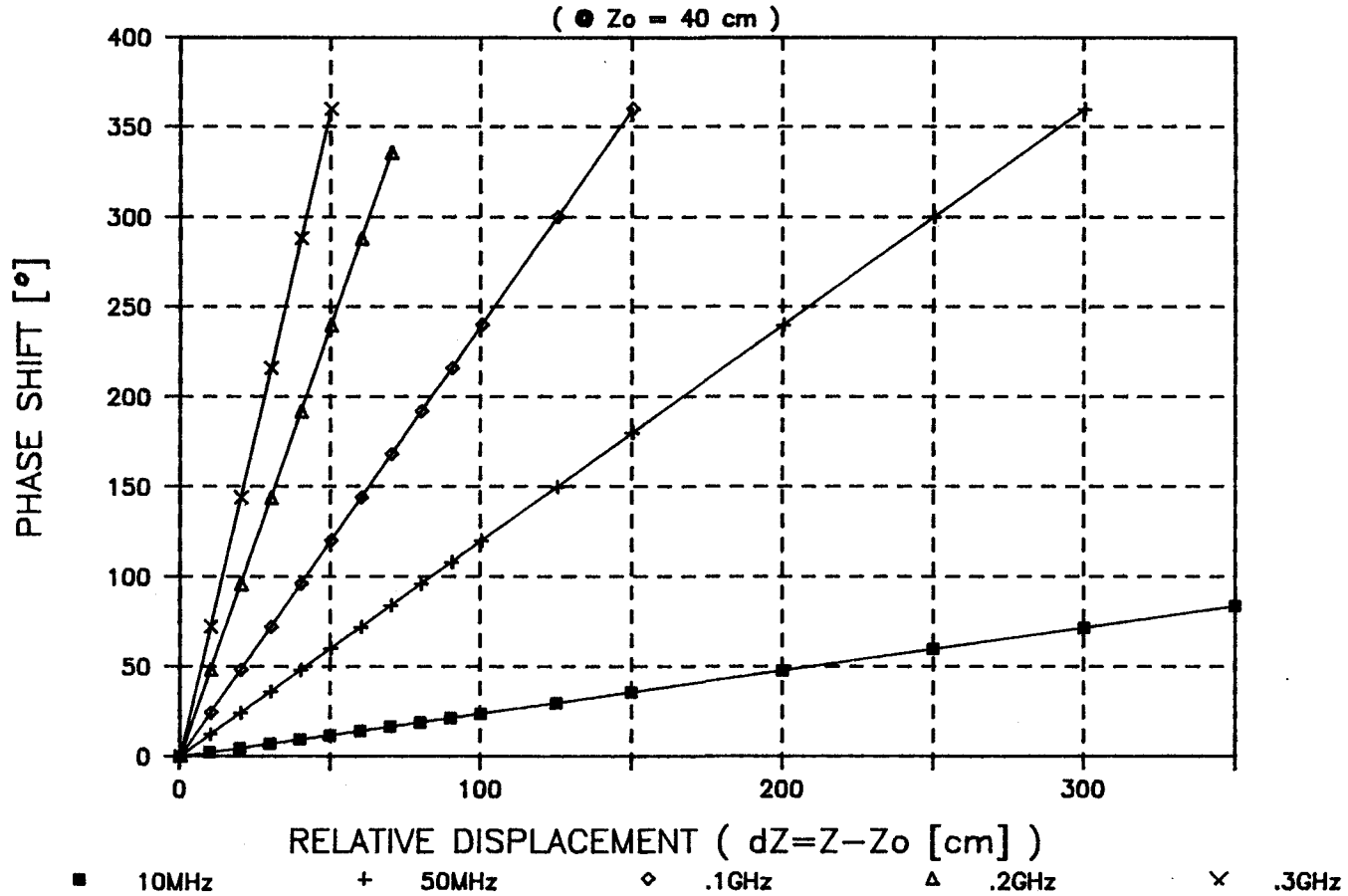


Fig. 3-9 Plot of displacement versus phase shift as a function of modulation frequency.

4. DISCUSSION

In the first stage of these experiments, a direct amplitude modulation of a semiconductor diode laser was performed. The direct amplitude modulation of a diode laser was shown to be a simple and convenient technique for generating a modulated light source. However, it presents several problems for applications such as the limitation of modulation frequency (from around 1 GHz [27] up to 20 GHz [29]) and difficulty of modulating at frequencies > 1 GHz with large amplitudes and mW power levels.

Direct amplitude modulation was achieved with the SHARP CD diode laser only up to 300 MHz ($> -3\text{dB}$), probably due to the RF electrical components in the drive circuit. Thus it is desirable to employ well shielded high frequency components and circuits in order to obtain a reliable, high performance system at high frequencies (> 1 GHz).

Although the laser beams are nearly collimated, the sensor system is capable of a very wide range of displacement measurements (using frequencies from 10 MHz - 300 MHz). The ratio of the photodetector surface area (A_{PD}) to the area of the returned signal laser beam spot size (A_S) could be another range variable parameter which could be utilized to measure wide range displacements. If

the photodetector has a very small surface area compared to the size of the beam spot, Eqn. (2-16) should be modified to Eqn. (4-1) with the area ratio ($\Gamma = A_{PD} / A_S$) which is limited to unity ($0 \leq \Gamma \leq 1$). The Γ cannot exceed unity since for $A_{PD} > A_S$ all the signal falls within the detector.

$$dz_{rms} = c / [4 \cdot \pi \cdot f_m \cdot \sqrt{2(\eta \cdot \Gamma \cdot P_S) / (h \cdot f_o \cdot BW)}] \quad (4-1)$$

A large area photodetector (UDT-PIN, 10D #274-1, whose surface diameter is measured as 10 mm) was tested to check whether or not the local oscillator beam and the signal beam are required to focus onto the same spot of the photodetector in order to generate the beat signal from the two light sources. The result was quite appealing in its application since it showed that it is not necessary to focus the beams on the same spot as long as they are on the photodetector surface.

One of the interesting aspects observed during the experiments was that the dual-frequency diode laser displacement sensor was so sensitive that it could be used to detect any small mechanical vibration. Any minute shock in the laboratory was detected on the oscilloscope as a floating DC level. This phenomenon was more significantly observable after passing the pre-amplification stage.

As stated in the introduction, the dual-frequency diode laser displacement sensor is not developed for absolute range measurement but was designed and tested in the laboratory to demonstrate its high resolution over a predetermined dynamic range of displacements. Although the phase shift caused by a displacement can be used to measure a range, the analysis of large phase shifts was not considered as much as the heterodyne signal power level which allows displacement measurement accuracy. In order to increase versatility of the dual-frequency diode laser displacement sensor, it will be necessary to employ optical components, such as a collecting lens and a beam splitter. As the sensor system becomes more sophisticated, it can be assigned to any environment to measure precision displacement. Therefore, optical components should be considered and studied for future development of displacement sensor design.

5. CONCLUSIONS

A dual-frequency diode laser displacement sensor was theoretically designed and experimentally tested. It was verified experimentally that the laser heterodyne technique is suitable for noncontact measurements of small displacement of reflecting objects. Although its noise characteristics are similar to those of conventional homodyne or heterodyne systems, the displacement sensor constructed has the remarkable advantage that the small displacement information of concern can be obtained from detection of the beat photocurrent between two amplitude modulated laser diodes. From an experimental point of view, this fact makes it very easy to get such information.

The sensor system does not require ultra-short pulses and consequently does not require high-cost electronics. This displacement measurement technique combined with a GaAlAs diode laser and Si photodetector represents a very cost-effective way to acquire accurate small-scale displacement measurements and maintain suitable accuracy for industrial applications. It can be applied to determine surface roughness, object profile, stress on a structure, and so on.

The sensor described in this thesis has noise-limited distance resolutions in the range of 50 nm to 1.4

um over dynamic ranges of 0.01 m to 3.5 m . The practical limitation will be how accurately can the phase shifts $d\phi$ be measured. While crude direct scope measurements have been done here, there are other sensitive techniques available such as lock-in detection and phase-locked loops which can provide much better resolution.

Large signal-to-noise ratio and high frequency modulation make this a versatile and powerful technique for the measurement and control of small displacement. The major advantages of this sensor system are its simple construction and its high resolution. It is also easy to operate.

A more detailed study and further experiments on the dual-frequency diode laser displacement sensor seem necessary to achieve higher performance. One of the important features to be investigated will be the phase error generated by temperature effects on the sensor system. Also, phase detection circuitry rather than phase difference measurement on a scope will yield better information on displacement measurements. Finally, computer modeling of the diode laser and photodetector could lead to a better understanding of direct amplitude modulation and of heterodyne detection and to better drive and detection circuits.

BIBLIOGRAPHY

- [1] "Optical Gauging of Surfaces," in "Optics in Engineering Measurement," Proc. SPIE vol.599, session 5, pp. 303-320, 1985
- [2] J. T. Luxon and D. E. Parker, "Industrial Lasers and Their Applications," Englewood Cliffs, NJ: Prentice-Hall, Inc., pp. 145-199, 1985.
- [3] J. F. Ready, "Industrial Applications of Lasers," New York, NY: Academic Press, Inc., pp. 247-335, 1978.
- [4] "Laser Radar Technology and Applications," Proc. SPIE, vol. 663, 1986.
- [5] M. Born and E. Wolf, "Principles of Optics," 3rd ed., Long Island City, NY: Pergamon Press, Inc., pp. 256-322, 1965.
- [6] R. Kingslake, "Applied Optics and Optical Engineering," vol.IV, Optical Instruments, Part I, Rochester, NY: Academic Press, Inc., pp. 309-361, 1967.
- [7] C. R. Munneryn, "A Simple Laser Interferometer," Appl. Opt. vol. 8, no. 4, pp. 827-828, 1969.
- [8] G. L. Bourdet and A. G. Orszag, "Absolute distance measurements by CO₂ laser multiwavelength interferometry," Appl. Opt. vol. 18, no. 2, pp. 225-227, 1979.
- [9] A. Thansandote, S. S. Stuchly, and J. S. Wight, "Microwave Interferometer for Measurements of Small Displacements," IEEE Trans. Instrum. Meas., vol. 31, no. 4, pp. 227-232, 1982.
- [10] G. Hartman and T. Nicholas, "An enhanced laser interferometer for precise displacement

- measurements," *Exp. Tech.* vol.11, no. 2, pp.24-26, 1987.
- [11] J.P. Monchalin "Optical Detection of Ultrasound," *IEEE Trans. Ultrason., Ferroelectrics, Freq. Contr.*, vol. UFFC-33, pp. 485-499, 1986.
- [12] Y. Ohtsuka and K. Itoh, "Two-frequency laser interferometer for small displacement measurements in a low frequency range," *Appl. Opt.*, vol. 18, no. 2, pp. 219-224, 1979.
- [13] K. H. Yang, L. Chen, and S. Y. Zhang, "Laser interferometer using a dual interference method," *Electron. Lett.* vol. 23, no. 13, pp. 699-700, 1987.
- [14] A. Sarrafzadeh-Khoei and J. C. Duke, Jr. "Non-contacting detection in ultrasonic nondestructive evaluation of materials: simple optical sensor and fiber-optic interferometric application," *Rev. Sci. Instrum.*, vol. 57, no. 9, pp. 2321-2325, 1986.
- [15] R. T. Bow and C. P. Wang, "Laser Phase-Detector And Counter For Fine Displacement Measurement," *Proc. Intern. Conf. on Lasers*, pp. 526-530, 1985.
- [16] G. Hausler and J. M. Herrmann, "Range sensing by shear-ing interferometry: influence of speckle," *Appl. Opt.* vol. 27, no. 22, pp. 4631-4637, 1988.
- [17] P. Juncar and J. Pinard, "Instrument to measure wave-numbers of cw and pulsed laser lines: The sigmameter," *Rev. Sci. Instrum.* vol. 53, no. 7, pp. 939-948, 1982.
- [18] K. Y. Lau and A. Yariv, "Ultra-High Speed Semiconductor Lasers," *IEEE J. Quantum Electron.*, vol. 21, pp. 121-138, 1985.
- [19] R. S. Tucker, "High-Speed Modulation of Semiconductor Lasers," *J. Lightwave Technol.*, vol. LT-1, pp. 1180-1192, Dec. 1985.

- [20] H. Olesen and G. Jacobsen, "A Theoretical and Experimental Analysis of Modulated Laser Fields and Power Spectra," IEEE J. Quantum Electron., vol. 16, no. 12, pp. 2069-2080, 1982.
- [21] A. Yariv, "Optical Electronics," 3rd ed., New York, NY: CBS College Publishing, pp. 345-363, 490-4494, 1985.
- [22] D. Welford and S. B. Alexander, "Magnitude and Phase Characteristics of Frequency Modulation in Directly Modulated GaAlAs Semiconductor Diode Lasers," J. Lightwave Technol., vol. LT-3, pp. 1092-1099, 1985.
- [23] J. J. Snyder, "Wide dynamic range optical power measurement using coherent heterodyne radiometry," Appl. Opt. vol. 21, no. 21, pp. 4465-4469, 1988.
- [24] M. I. Skolnik, "Introduction to Radar Systems," 2nd ed., New York, NY: McGraw-Hill, 1980.
- [25] M. Ross, "Laser Receivers; Devices, Techniques, Systems," New York, NY: John Wiley & Sons, Inc., pp. 98-130, 1966.
- [26] R. W. Boyd, "Radiometry and the Detection of Optical Radiation," New York, NY: John Wiley & Sons, Inc., pp. 119-136, 1983.
- [27] SHARP Corp., "Laser Diode User's Manual," Sept. 1988.
- [28] K. A. Jones, "Introduction to Optical Electronics," New York, NY: Harper & Row, Publishers, Inc., pp. 27 (Figure 1-13), 1987.
- [29] T. Sueta and M. Izutsu, "Integrated Optic Devices for Microwave Applications," IEEE Trans. Microwave Theory Tech. vol. MTT-38, no. 5, pp. 477-482. 1990.